

Research article

Sonophore labeled RGD: a targeted contrast agent for optoacoustic imaging



Katja Haedicke^a, Christian Brand^b, Murad Omar^{c,d}, Vasilis Ntziachristos^{c,d},
Thomas Reiner^b, Jan Grimm^{a,b,e,*}

^a Molecular Pharmacology Program, Memorial Sloan Kettering Cancer Center, New York, NY, USA

^b Department of Radiology, Memorial Sloan Kettering Cancer Center, New York, NY, USA

^c Chair of Biological Imaging, Technische Universität München, Munich, Germany

^d Institute of Biological and Medical Imaging, Helmholtz Zentrum München, Neuherberg, Germany

^e Weill Cornell Medical College, Pharmacology Program and Department of Radiology

ARTICLE INFO

Article history:

Received 17 October 2016

Received in revised form 20 January 2017

Accepted 1 March 2017

Keywords:

Optoacoustic imaging

Photoacoustic imaging

Black hole quencher

RGD peptide

Contrast agent

Sonophore

ABSTRACT

Optoacoustic imaging is a rapidly expanding field for the diagnosis, characterization, and treatment evaluation of cancer. However, the availability of tumor specific exogenous contrast agents is still limited. Here, we report on a small targeted contrast agent for optoacoustic imaging using a black hole quencher[®] (BHQ) dye. The sonophore BHQ-1 exhibited strong, concentration-dependent, optoacoustic signals in phantoms, demonstrating its ideal suitability for optoacoustic imaging. After labeling BHQ-1 with cyclic RGD-peptide, BHQ-1-cRGD specifically bound to $\alpha_v\beta_3$ -integrin expressing glioblastoma cell spheroids *in vitro*. The excellent optoacoustic properties of BHQ-1-cRGD could furthermore be proven *in vivo*. Together with this emerging imaging modality, our sonophore labeled small peptide probe offers new possibilities for non-invasive detection of molecular structures with high resolution *in vivo* and furthers the specificity of optoacoustic imaging. Ultimately, the discovery of tailor-made sonophores might offer new avenues for various molecular optoacoustic imaging applications, similar to what we see with fluorescence imaging.

© 2017 The Authors. Published by Elsevier GmbH. This is an open access article under the CC BY-NC-ND license (<http://creativecommons.org/licenses/by-nc-nd/4.0/>).

1. Introduction

Optoacoustic imaging is an expanding research field, especially for non-invasive imaging and characterization of tumors, enabling a better understanding of cancer biology and treatment outcomes [1,2]. This modality images the absorption of pulsed light by fluorochromes and biomolecules deep in biological tissues via the generated ultrasound waves. This passive detection of optical absorption enables a sensitive detection of biological processes from deep inside the tissue. After the excitation of a contrast agent by a nanosecond pulsed laser of a certain wavelength, a thermo-elastic expansion of these molecules is induced during the emission process, which leads to the generation of detectable ultrasound waves from the illuminated area [3]. The advantage compared to optical imaging is that the resolution in optoacoustics

is not affected by light attenuation due to tissue scattering as it is defined by acoustic propagation and acoustic scattering. Therefore, a preservation of the signal strength and resolution is given even in deeper tissue layers [3,4].

Also, recently a high-resolution optoacoustic imaging device was developed, termed raster-scan optoacoustic mesoscopy (RSOM). RSOM was introduced to overcome given limitations of other optoacoustic technologies like, for example, limited resolution. This prototype scanner revealed the tumor vascular network and its development in sub-millimeter high-resolution non-invasively [5]. Here, the endogenous contrast of hemoglobin was used to depict single vessels. Optoacoustic mesoscopy could also reveal skin layers as well as insights into melanin content and blood oxygenation in human skin *in vivo* [6–8]. However, next to the use of these endogenous contrasts, the availability of tumor specific exogenous contrast agents was still limited.

On the basis of the above it becomes clear that for further analysis of different targets and receptors and thus for gaining more specific information about tumor biology and disease-associated processes, the inclusion of exogenous contrast agents for optoacoustic imaging is indispensable. Especially near-infrared

* Corresponding author. 1275 York Ave, Box 248, New York, NY 10065.

E-mail addresses: haedick@mskcc.org (K. Haedicke), brand@mskcc.org (C. Brand), murad.omar@tum.de (M. Omar), v.ntziachristos@tum.de (V. Ntziachristos), reinert@mskcc.org (T. Reiner), grimmj@mskcc.org (J. Grimm).

fluorescent dye-labeled probes are widely used in optical imaging to generate a visual signal after light excitation [9,10]. However, these dyes mainly emit absorbed energy in the form of fluorescence, making only a partial amount of the energy available for thermoelastic expansion, which results in the generation of a weaker optoacoustic signal. Therefore, a group of dyes called dark quenchers, so far mainly used to quench fluorescence of other dyes in the study of biomolecule dynamics [11–13], is highly promising for the design of contrast agents in optoacoustic imaging. They emit absorbed energy mainly as heat, by a non-radiative conversion of the light energy, which is accompanied by the formation of acoustic waves. As a result, the thermoelastic expansion is expected to be larger for quenchers than for light emitting fluorochromes [14]. While dark quenchers were used as molecular beacon-like probes in the past [15,16], these quencher dyes were never used as a standalone sonophore contrast agent in optoacoustic imaging so far.

Here, we introduce the first sonophore labeled targeted probe using cyclic RGD (BHQ-1-cRGD). By means of embedding a dilution series of the quencher dye into agarose phantoms, we demonstrated the suitability of BHQ-1 for the generation of a strong optoacoustic signal as a first prerequisite for our study. After successful labeling with the RGD peptide, the binding specificity of our probe to tumor cells was investigated using glioblastoma cell spheroids. Furthermore, we applied the quencher dye subcutaneously *in vivo* to demonstrate the ability of the generation of an optoacoustic signal by BHQ-1 as a first proof of concept. The specific accumulation of BHQ-1-cRGD in glioblastoma tumors *in vivo* was investigated as a final step.

2. Material and Methods

2.1. Cell line and animals

Human glioblastoma cells (U-87 MG) were obtained from ATCC® (VA, US) and cultured in Eagle's Minimum Essential Medium (Corning Cellgro, VA, US) containing 10% FBS, 1% Penicillin/Streptavidin solution, 2 mM L-glutamine, 1 mM sodium pyruvate and 0.075% (w/v) sodium bicarbonate. They were incubated in a humidified 5% CO₂ atmosphere and used between passages 8 and 15.

For *in vivo* experiments, 6–8 week old female Hsd:Atymic Nude-Foxn1^{tmu} mice were purchased from Envigo (IN, US). All animal experiments were performed in accordance with institutional guidelines and approved by the IACUC of MSK, and followed NIH guidelines for animal welfare.

2.2. Synthesis and characterization of BHQ-1-cRGD

To a stirring solution of cyclic RGD (*cyclo*(Arg-Gly-Asp-D-Phe-Lys), 1.0 mg, 1.66 μmol, 1.0 eq., Peptides international, KY, US) in anhydrous DMF (200 μL) a solution of BHQ-1 *N*-hydroxysuccinimide (NHS) ester (1.2 mg, 2.0 μmol, 1.2 eq., Biosearch technologies, CA, US) in anhydrous DMF (200 μL) and triethylamine (1.2 μL, 8.0 μmol, 4.8 eq) was added sequentially. The resulting reaction solution was stirred for 4 h at room temperature. Purification by high performance liquid chromatography (HPLC) (C18, 10% to 100% of acetonitrile over 10 min, then 100% of acetonitrile until 18 min, 1.0 mL/min) yielded BHQ-1-cRGD (1.5 mg, 1.4 μmol, 82%) as a black solid. The purity of BHQ-1-cRGD was analyzed by performing analytical HPLC ($t_r = 11.0$ min, >97%). The identity of the product (C₃₅H₆₇N₁₅O₁₁, MW: 1090.21 g/mol) was verified by electrospray ionization mass spectrometry (ESI(+): m/z (%) 546.70 (100) [M+2H]²⁺, 1090.40 (25) [M+H]⁺). The absorbance spectra of BHQ-1 and BHQ-1-cRGD were measured in ethanol using spectrophotometry from 250 nm to 750 nm.

2.3. Optoacoustic imaging

For imaging, we used our high-resolution raster-scan optoacoustic mesoscopy (RSOM) prototype scanner in epi-illumination mode [17]. This technology was obtained in a collaboration from the Institute for Biological and Medical Imaging at the Helmholtz Zentrum Munich (Germany). The scanner illuminates the tissue with a fast monochromatic nanosecond laser (1 ns, 2 kHz, 1 mJ pulse energy at 532 nm). The laser light was coupled to the sample using a three arm fiber bundle which is combined with the ultrasound detector into a single scan unit. The optoacoustic signals were measured with a 50 MHz spherically focused detector and a bandwidth of 5–80 MHz. Furthermore, the signals were amplified with a 63 dB low noise amplifier and digitized using a fast 12 bit data acquisition card. The scan was performed in a continuous-discrete manner and with a raster step size of 20 μm. The usual scan took 1.30 minutes for a field of view of 8 × 8 mm² and the maximum depth was about 2 mm, limited by the penetration depth of 532 nm photons in tissue.

The raw signals were transformed to the computer on which they were later reconstructed using beam forming. Before reconstruction, the signals were divided into two sub-bands: low frequencies 5–25 MHz and high frequencies 25–80 MHz as described before [5]. In short, we divided the frequency bands such that the relative bandwidth $BW\% = BW/f_c$, where BW is bandwidth of sub-band and f_c is the central frequency, which is the same for all the sub-bands. These sub-bands were later on separately reconstructed and overlaid using different colors (red=low frequencies, green=high frequencies). For all samples, the same sub-bands were used, which were optimized before in order to get as low ringing effect as possible by keeping the same relative bandwidth in all of the sub-bands. For the reconstruction a speed of sound of 1540 m/s has been used for all samples after performing measurements in ~34 °C warm water and the reconstruction has been performed with voxel sizes of 20 × 20 × 5 μm³. Finally, the Hilbert transform was applied to the reconstructed volume along the depth, i.e. the z -axis to remove the negative values and to obtain the profile of the signal generating object. The images were further processed using a Wiener and a Median filter to improve the signal to noise ratio. For visualization we took the maximum intensity projection of the three-dimensional volume.

2.4. Agarose phantom studies of BHQ-1

The quencher dye BHQ-1 (10 mM in DMSO) was embedded at different concentrations (0 μM to 500 μM) into 1% agarose phantoms (10 μL, preheated at 70 °C). Agarose drops containing the agent were placed next to each other into a 1% agarose-coated petri dish and covered with water to enable ultrasound signal detection. The experiment was done in triplicates and RSOM was performed as described under 2.3 but without dividing the detected ultrasound frequencies into smaller sub-bands during the reconstruction process. The generated images were analyzed using ImageJ and regions of interest (ROIs) were manually drawn over the detected phantom signals to quantify the optoacoustic signals of the BHQ-1 dilution series. For analysis, the mean pixel value of each ROI was used.

2.5. RSOM of BHQ-1-cRGD in U-87 cell spheroids in vitro

U-87 cell spheroids were grown by transferring 1 × 10⁶ U-87 cells, raised in normal growth medium, into a 1% agarose-coated cell culture flask (75 cm²) and incubated for about one week. After they reached sizes of approximately 0.6 to 1.0 mm, 12 spheroids were collected and transferred into agarose-coated wells of a

96-well plate. Representative images of the spheroids were taken using a light microscope. For 2 hours, 4 spheroids were incubated with 50 μ l cell culture medium without the probe, with 50 μ M BHQ-1-cRGD or with 50 μ M BHQ-1-cRGD and a 100-fold excess (5 mM) of free cyclic RGD, respectively. Afterwards, the spheroids were gently washed for three times with PBS, embedded in 1% agarose in a petri dish and covered with water. After performing RSOM as described under 2.3 without dividing the ultrasound frequencies into smaller sub-bands during the reconstruction process, the spheroid images were analyzed quantitatively using manual ROI measurement in ImageJ. Here, one ROI was placed over the spheroid and a second one over the background. The signal to noise ratio was calculated for each spheroid using the mean pixel value of each ROI.

2.6. RSOM of BHQ-1 in mouse footpad *in vivo*

All mice were anesthetized using 2% isoflurane. For imaging the quencher dye *in vivo*, 10 nmol BHQ-1 solution were injected subcutaneously into the footpad of 3 mice. The mouse was then placed in a pre-warmed water bath on a mouse bed keeping the head of the animal above water level. The foot of the mouse was stabilized under water with tape to keep it in a static position for the measurement procedure. The feet were measured before and directly after injection using RSOM as described under 2.3. Quantitative analysis was done in ImageJ by manually placing a ROI over the injection site of each foot as well as over the background blood vessels in the footpad. The mean pixel value of each ROI was used for the analysis of the two sub-bands and the overlay image.

2.7. RSOM of BHQ-1-cRGD in U-87 tumors *ex vivo*

U-87 tumors were implanted into 6 mice by injecting 2×10^6 U-87 cells in 100 μ l 1:1 matrigel:medium subcutaneously into the

lower left back. After tumors reached a diameter of approximately 6 mm, one group of 3 mice were injected intravenously with 50 nmol BHQ-1-cRGD in 150 μ l sodium chloride and a second group of 3 mice with 150 μ l sodium chloride only as a control. After 2 hours, mice were anesthetized using 2% isoflurane and perfused via the heart using PBS until all blood was removed from the body. The tumors were excised, placed in ultrasound gel in a petri dish, covered with a transparent foil and with water and imaged using RSOM as described under 2.3. Analysis was done using ImageJ by generating a profile plot for one representative tumor of each animal group.

2.8. Statistical analysis

The data are shown as mean values and error bars represent the standard deviation. The statistical significance of the data was analyzed using an unpaired Student's *t*-test in GraphPad Prism 6.0. A P-value of 0.05 or less was considered to be statistically significant.

3. Results

3.1. Synthesis and characterization of BHQ-1-cRGD

The synthesis of the black hole quencher[®] labeled peptide probe is shown in Fig. 1A. In the presence of triethylamine, the NHS ester-activated BHQ-1 was successfully conjugated to the primary amine of the cyclic RGD and the final product was isolated in 82% yield after HPLC purification. Identity and purity of BHQ-1-cRGD were validated successfully through mass spectrometry and analytical HPLC resulting in a molecular weight of 1,090 g/mol (Fig. 1B and C). The absorption spectrum of BHQ-1 alone as well as of BHQ-1-cRGD peaked at 515 nm, suggesting that the labeling procedure did not change the optical properties of the black quencher (Fig. 1D). Additionally, the spectrum of BHQ-1-cRGD

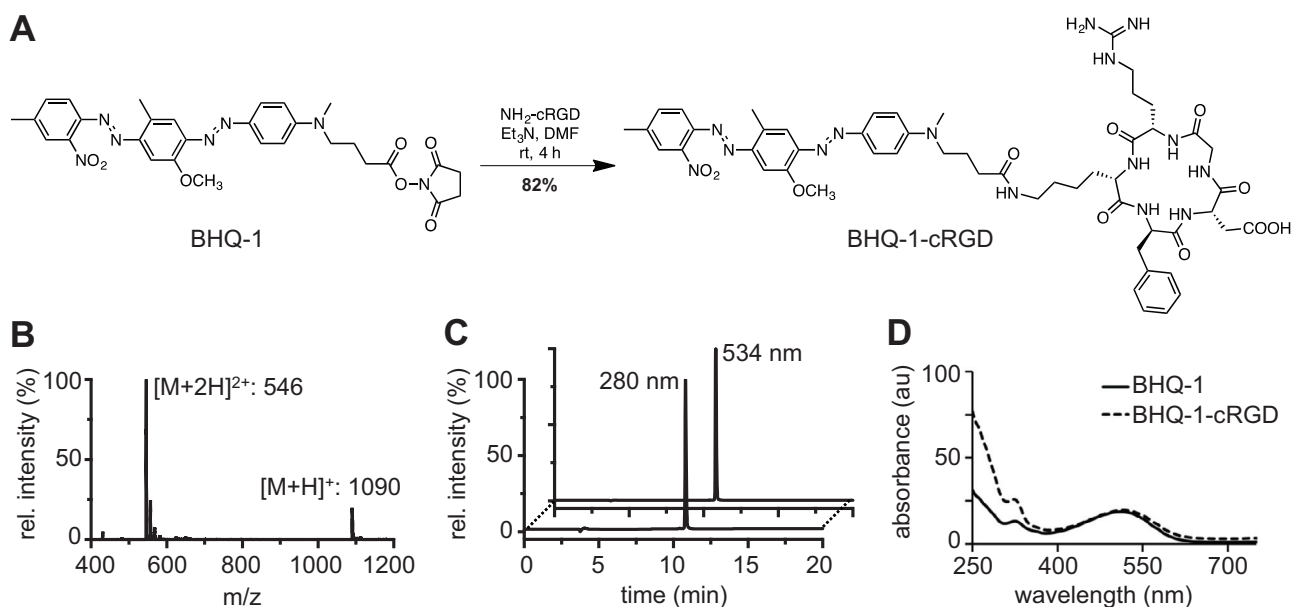


Fig. 1. Synthesis and chemical properties of BHQ-1-cRGD as a promising contrast agent for optoacoustic imaging. **A:** Synthesis of BHQ-1-cRGD through NHS ester amid bond formation. BHQ-1-NHS was labeled with NH_2 -cRGD using Et_3N and DMF while incubating for 4 hours at room temperature; yield = 82%. **B:** Mass spectrometry analysis (positive polarized) of BHQ-1-cRGD confirmed the calculated molecular weight of 1,090 g/mol. **C:** Analytical HPLC chromatogram of BHQ-1-cRGD displays purity of the probe in two wavelengths while 280 nm shows absorbance of the RGD peptide and 534 nm of BHQ-1. **D:** Absorption spectrum of BHQ-1 (solid line) and BHQ-1-cRGD (dotted line) peaked at 515 nm and additionally at 280 nm for the RGD-labeled probe.

showed another peak at 280 nm, representing the RGD peptide in the probe.

3.2. RSOM of BHQ-1 in agarose-phantoms

After embedding BHQ-1 into agarose phantoms, a visible change in the color of the phantoms was detected from transparent to purple with increasing concentration of BHQ-1 from 0 μM to 500 μM (Fig. 2A). Furthermore, an increasing optoacoustic signal was detected with increasing concentration of BHQ-1 using RSOM (Fig. 2B). Stronger signals are reflected in a more intense green compared to lower signals. The quantitative analysis of the RSOM image of the BHQ-1 phantoms confirmed the optical findings and revealed increasing mean optoacoustic signals from 4.8 ± 2.4 AU (arbitrary units) out of the 0 μM phantom up to 73.5 ± 11.2 AU from the 500 μM phantom (Fig. 2C).

3.3. RSOM of BHQ-1-cRGD in U-87 spheroids in vitro

A strong optoacoustic signal could be detected after incubating U-87 glioblastoma cell spheroids with the BHQ-1-cRGD probe for 2 hours (Fig. 3A). Almost no signal appeared in the native spheroids without the probe and a comparatively low optoacoustic signal was depicted after incubation with a 100-fold excess of free cyclic RGD simultaneously to the BHQ-1-cRGD probe. A comparison of the RSOM images with the white light pictures highlighted that a high binding of BHQ-1-cRGD onto cells results in a stronger optoacoustic signal. The quantitative analysis confirmed the successful binding of BHQ-1-cRGD onto U-87 cells at a concentration of 50 μM with a signal to noise ratio of 11.0 ± 2.8 (Fig. 3B). In comparison, the native spheroids themselves did not generate an optoacoustic signal above background noise with a statistically significant lower ratio of 1.0 ± 0.0 ($P \leq 0.0005$). Furthermore, the 100-fold excess of cyclic RGD blocked the binding of BHQ-1-cRGD to the spheroids significantly with a signal to noise ratio of only 4.8 ± 2.7 ($P \leq 0.05$).

3.4. RSOM of BHQ-1 in mouse footpad in vivo

Following a subcutaneous injection of 10 nmol BHQ-1 into the mouse footpad, a strong optoacoustic signal could be detected at the injection site compared to the homogeneous signal before the application (Fig. 4A). At the same time, the relative intensity of the signal generated by hemoglobin in the blood vessels of the footpad decreased rapidly compared to before the injection. A stronger optoacoustic signal could be seen for both the low as well as the

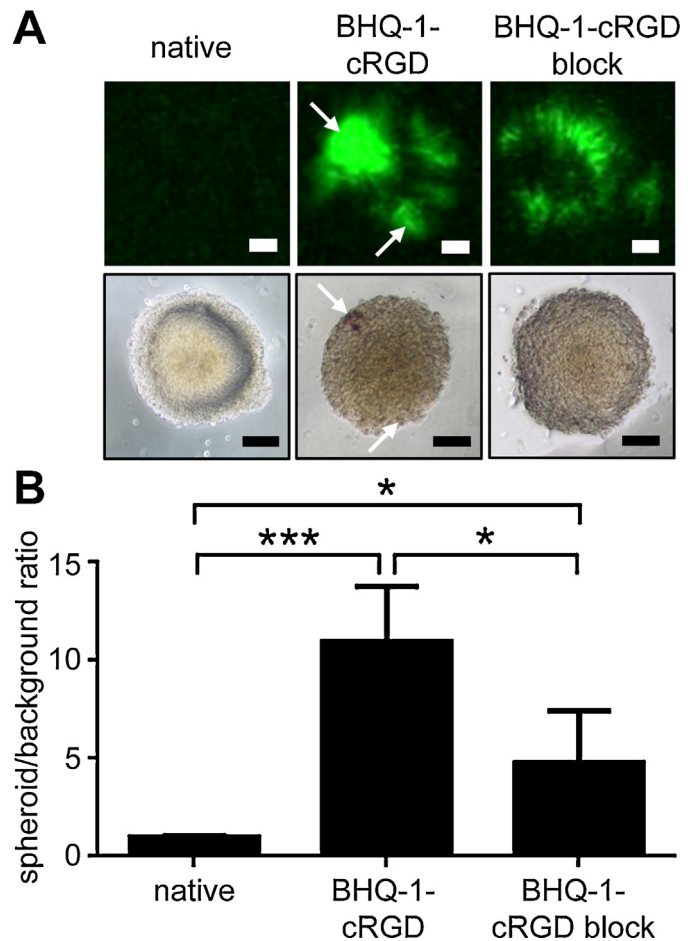


Fig. 3. *In vitro* RSOM of U-87 cell spheroids after incubation with BHQ-1-cRGD confirmed the specificity of the probe. **A:** Upper row: RSOM images of U-87 spheroids 2 h after incubation without (native) and with 50 μM BHQ-1-cRGD as well as 50 μM BHQ-1-cRGD with 100-fold excess (5 mM) of free cyclic RGD (block) in medium showed specific binding of the probe (arrows). Lower row: light microscopy images of representative U-87 cell spheroids; scale = 200 μm . **B:** Quantitative analysis of the detected optoacoustic signal in U-87 spheroids clarifies the specificity of BHQ-1-cRGD; n = 4; *** $P \leq 0.0005$; * $P \leq 0.05$.

high frequencies and also on the overlay image of all frequencies. A 3D-surface plot of the footpad before and after injection confirmed these observations (Fig. 4A). The quantitative analysis revealed an almost 5-times higher optoacoustic signal at the injection site with

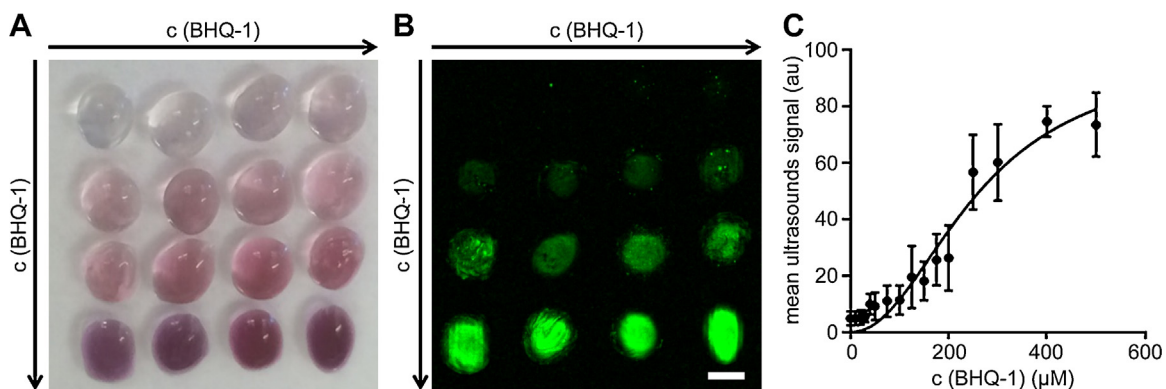


Fig. 2. RSOM of a dilution series of BHQ-1 in agarose phantoms proved the suitability of the quencher dye for optoacoustic imaging. **A:** White light image of a dilution series of BHQ-1 in agarose phantoms (0 μM to 500 μM from upper left to lower right). **B:** RSOM image (optoacoustic signal) of the agarose phantoms with the dilution series of BHQ-1 (0 μM to 500 μM from upper left to lower right) reflects a more intense green with increasing BHQ-1 concentration; scale = 2 mm. **C:** Quantitative analysis of the detected optoacoustic signal in BHQ-1 agarose phantoms reveals an increasing signal with increasing BHQ-1 concentration; n = 3.

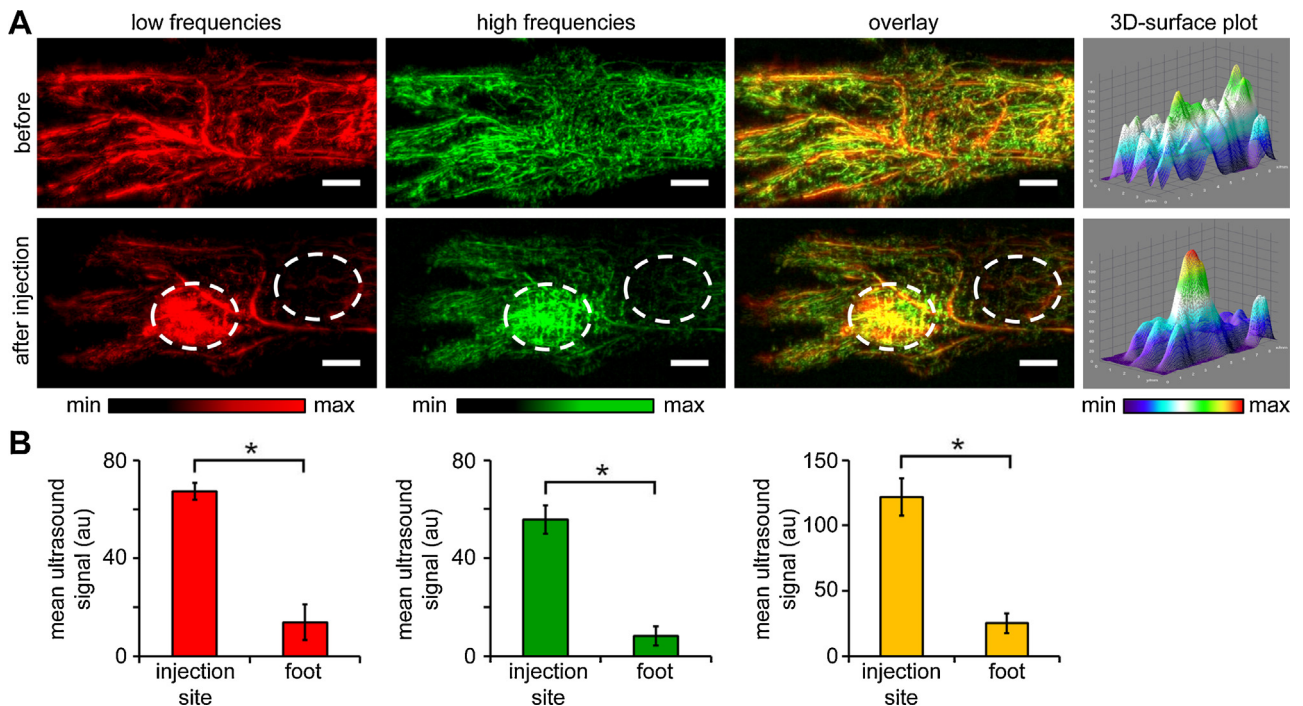


Fig. 4. RSOM before and after subcutaneous injection of 10 nmol BHQ-1 into mouse footpad proves optoacoustic properties of the black quencher *in vivo*. **A:** RSOM images of mouse footpad before and after subcutaneous injection of BHQ-1; red = low frequencies (big structures); green = high frequencies (small structures); yellow = overlay; white circle = injection site and foot background; scale = 1 mm. Right: 3D-surface plot of the detected optoacoustic signal of the footpad; blue = low signal; red = high signal. **B:** Quantitative analysis of the detected optoacoustic signal at the injection site compared to the footpad background illustrated the strong optoacoustic signal of BHQ-1 *in vivo*; n = 3; * P < 0.0005.

121.6 ± 14.2 AU compared to the surrounding footpad vessels with only 25.2 ± 7.7 AU for the overlay image of all detected frequencies (P < 0.0005, Fig. 4B, yellow). The same trend was observed for the separated low frequencies (5–25 MHz, red) with values of 67.2 ± 3.4 AU versus 13.9 ± 7.2 AU and the high frequencies (25–80 MHz, green) with 55.6 ± 5.7 AU versus 8.3 ± 3.9 AU respectively (P < 0.0005).

3.5. RSOM of BHQ-1-cRGD in U-87 tumors ex vivo

After intravenous injection of 50 nmol BHQ-1-cRGD into 3 mice followed by perfusion, a clear optoacoustic signal could be detected in these tumors compared to the ones with only sodium chloride as a control (Fig. 5A). The representative tumors show a clear trend for the specific accumulation of our probe in the U-87 tumors. The poor signal in the sodium chloride tumors indicates the effective wash out of the blood by the perfusion. By drawing a line through the tumors, a histogram plot of the gray values could be generated, showing much higher optoacoustic values in the BHQ-1-cRGD injected mouse compared to the sodium chloride injected control animal (Fig. 5B). The strong signals in the BHQ-1-cRGD tumor show saturated values in some areas, meaning that the generated optoacoustic signals in these regions are extremely strong. The saturation originates from the raw signals due to the used back projection, which is a linear algorithm and used for the reconstruction process. It is propagated to the final reconstructed image which is why these saturated values appear.

4. Discussion

In this study we showed that our sonophore labeled RGD probe offers excellent capabilities for a targeted imaging of $\alpha_v\beta_3$ -integrin expressing tumors using optoacoustic imaging. As the availability of specific exogenous contrast agents is still limited in the field of

optoacoustics, our newly designed agent will pave the way for an innovative group of sonophore labeled probes, enabling a non-invasive detection of molecular structures with a high resolution *in vivo*.

Compared to other probes which are momentarily used for optoacoustics [18], our small peptide based contrast agent offers several advantages. While gold nanostructures like nanorods or nanoparticles have been utilized as contrast agents for optoacoustic imaging [19–22], a small peptide based contrast agent like BHQ-1-cRGD can offer better pharmacokinetic and pharmacodynamic properties than nanoparticles due to the smaller size, resulting in better biocompatibility. Our approach also circumvents the use of heavy metals in the body, which are applied with many other nanoparticle formulations. Furthermore, due to the fast clearance of RGD compounds from the body, the probe has no adverse accumulation in unwanted sites and thus is specific only to targets expressing high amounts of $\alpha_v\beta_3$ -integrin, such as tumors. Since RGD-peptides are already widely used in the field of optical imaging [23,24], are non-toxic and highly specific to $\alpha_v\beta_3$ -integrin over-expression, our agent could be applied rapidly in further studies or even translated for clinical applications. Moreover, the synthesis of the contrast agent was performed in one-step with a high yielding of 82%. Purification of the compound was facile without the need for further coating of the compound, as required for nanoparticle to improve biocompatibility.

The concentration dependent increase of the optoacoustic signal in agarose phantoms showed high sensitivity of this imaging technology. Optimization of the quencher dye properties to a higher absorption of light or a greater thermoelastic expansion can further improve the quality of the sonophore. Due to the use of a quencher, the absorbed energy is already predominantly emitted in form of heat. There is no loss of energy for the generation of fluorescence, meaning that the thermoelastic expansion of the molecules and thus the generation of photoacoustic signals are

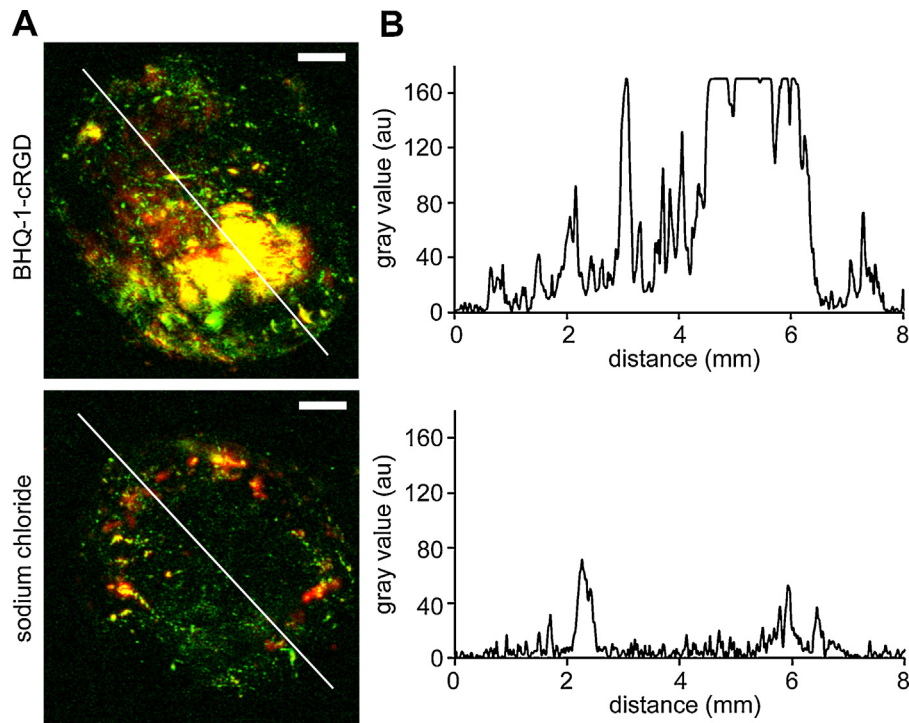


Fig. 5. RSOM of U-87 tumors *ex vivo* after intravenous injection of BHQ-1-cRGD and sodium chloride shows a clear trend for accumulation of our probe *in vivo*. **A:** Representative RSOM images of U-87 tumors *ex vivo* at 2 hours after intravenous injection of either 50 nmol BHQ-1-cRGD or sodium chloride only followed by a perfusion of the mouse using PBS; red = low frequencies (big structures); green = high frequencies (small structures); yellow = overlay; white line = line for profile plot. **B:** Profile plot through the U-87 tumors after BHQ-1-cRGD (top) or sodium chloride (bottom) injection.

promisingly higher. Another way to improve the signal outcome would be the encapsulation of the quencher into liposomes, thus offering a higher density of quencher at one spot and a better signal in the tumor as could already be shown in optoacoustic imaging using indocyanine green (ICG) encapsulated in PEGylated liposomes [25].

The binding of BHQ-1-cRGD was highly specific as we could show by using glioblastoma cell spheroids *in vitro*. The attachment of the sonophore to the RGD peptide did not change its specificity to the integrins. Even a small spheroid with a low number of cells could be detected, drawing the conclusion that also small size tumors can be illustrated with our contrast agent *in vivo*, making it ideal for tumor diagnostic or even metastases detection. Metastases detection has already been carried out using optoacoustic imaging [26,27], showing that this modality is capable of depicting small lesions within the body. Our sonophore labeled small peptide probe combined with the high resolution of RSOM can considerably improve this detection.

Further experiments showed a strong optoacoustic signal of the quencher dye as well as a specific detection of $\alpha_v\beta_3$ -integrin expressing glioblastoma tumors *in vivo*. In this context, additional experiments are necessary with the prospective availability of a suitable multispectral laser which could aid in distinguish endogenous signals from our exogenous contrast agent. We designed our probe to make it specific for the targeting of $\alpha_v\beta_3$ -integrin expressing tumors, including glioblastoma [28]. As a wide variety of tumors express integrins, the field of application is tremendous [29,30]. This means that also our sonophore labeled small peptide probe can be widely used in molecular imaging of tumors. It is also conceivable to use the sonophore with other targeting molecules, broadening its applicability.

5. Conclusion

In summary, our sonophore labeled peptide based contrast agent BHQ-1-cRGD showed a high suitability for optoacoustic imaging *in vitro* as well as *in vivo* with the generation of strong optoacoustic signals. Up to now, the availability of tumor specific exogenous contrast agents for optoacoustic imaging is limited. Therefore, this is the first step towards a new class of imaging probes in the field of optoacoustics. Sonophores can significantly propel the applicability of optoacoustic imaging and increase in conjunction with suitable imaging agents target precision for the detection of molecular structures *in vivo*. In combination with this fairly new imaging modality, this group of contrast agents is very promising for the investigation of tumor biology as well as cancer treatment efficacy in a non-invasive and high-resolution manner.

Funding

This work was supported in parts by the National Institute of Health (NIH) [R01EB014944 grant to Jan Grimm], the MSKCC NIH Core Grant [P30-CA008748] and the Wade F. B. Thompson Foundation Grant.

Conflict of Interest statement

K. Haedicke, C. Brand, M. Omar, T. Reiner and J. Grimm declare that there are no conflicts of interest. V. Ntziachristos is a shareholder in iThera Medical GmbH and therefore has financial interests.

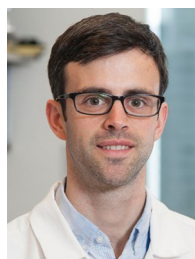
References

- [1] Y. Liu, L. Nie, X. Chen, Photoacoustic Molecular Imaging: From Multiscale Biomedical Applications Towards Early-Stage Theranostics, Trends in biotechnology (2016).
- [2] A. Taruttis, G.M. van Dam, V. Ntziachristos, Mesoscopic and macroscopic optoacoustic imaging of cancer, Cancer research 75 (8) (2015) 1548–1559.
- [3] V. Ntziachristos, D. Razansky, Molecular Imaging by Means of Multispectral Optoacoustic Tomography (MSOT), Chemical reviews 110 (5) (2010) 2783–2794.
- [4] D. Razansky, A. Buehler, V. Ntziachristos, Volumetric real-time multispectral optoacoustic tomography of biomarkers, Nat Protoc 6 (8) (2011) 1121–1129.
- [5] M. Omar, M. Schwarz, D. Soliman, P. Symvoulidis, V. Ntziachristos, Pushing the optical imaging limits of cancer with multi-frequency-band raster-scan optoacoustic mesoscopy (RSOM), Neoplasia 17 (2) (2015) 208–214.
- [6] J. Aguirre, M. Schwarz, D. Soliman, A. Buehler, M. Omar, V. Ntziachristos, Broadband mesoscopic optoacoustic tomography reveals skin layers, Optics letters 39 (21) (2014) 6297–6300.
- [7] M. Schwarz, A. Buehler, J. Aguirre, V. Ntziachristos, Three-dimensional multispectral optoacoustic mesoscopy reveals melanin and blood oxygenation in human skin in vivo, Journal of biophotonics (2015).
- [8] M. Schwarz, M. Omar, A. Buehler, J. Aguirre, V. Ntziachristos, Implications of ultrasound frequency in optoacoustic mesoscopy of the skin, IEEE transactions on medical imaging 34 (2) (2015) 672–677.
- [9] K. Umezawa, D. Citterio, K. Suzuki, New trends in near-infrared fluorophores for bioimaging, Analytical sciences: the international journal of the Japan Society for Analytical Chemistry 30 (3) (2014) 327–349.
- [10] S. Luo, E. Zhang, Y. Su, T. Cheng, C. Shi, A review of NIR dyes in cancer targeting and imaging, Biomaterials 32 (29) (2011) 7127–7138.
- [11] B. Simard, B. Tomanek, F.C.J.M. van Veggel, A. Abulrob, Optimal dye-quencher pairs for the design of an “activatable” nanoprobe for optical imaging, Photoch Photobio Sci 12 (10) (2013) 1824–1829.
- [12] J. Chen, A. Tsai, A. Petrov, J.D. Puglisi, Nonfluorescent quenchers to correlate single-molecule conformational and compositional dynamics, Journal of the American Chemical Society 134 (13) (2012) 5734–5737.
- [13] A. Chevalier, C. Massif, P.Y. Renard, A. Romieu, Bioconjugatable Azo-Based Dark-Quencher Dyes: Synthesis and Application to Protease-Activatable Far-Red Fluorescent Probes, Chem-Eur J 19 (5) (2013) 1686–1699.
- [14] J. Levi, S.R. Kothapalli, T.J. Ma, K. Hartman, B.T. Khuri-Yakub, S.S. Gambhir, Design, Synthesis, and Imaging of an Activatable Photoacoustic Probe, Journal of the American Chemical Society 132 (32) (2010) 11264–11269.
- [15] A. Maeda, J. Bu, J. Chen, G. Zheng, R.S. DaCosta, Dual in vivo photoacoustic and fluorescence imaging of HER2 expression in breast tumors for diagnosis, margin assessment, and surgical guidance, Molecular imaging 13 (2014).
- [16] K. Yang, L. Zhu, L. Nie, X. Sun, L. Cheng, C. Wu, G. Niu, X. Chen, Z. Liu, Visualization of protease activity in vivo using an activatable photo-acoustic imaging probe based on CuS nanoparticles, Theranostics 4 (2) (2014) 134–141.
- [17] M. Omar, D. Soliman, J. Gateau, V. Ntziachristos, Ultrawideband reflection-mode optoacoustic mesoscopy, Optics letters 39 (13) (2014) 3911–3914.
- [18] J. Weber, P.C. Beard, S.E. Bohndiek, Contrast agents for molecular photoacoustic imaging, Nature methods 13 (8) (2016) 639–650.
- [19] J. Vonnemann, N. Beziere, C. Bottcher, S.B. Riese, C. Kuehne, J. Dernerde, K. Licha, C. von Schacky, Y. Kosanke, M. Kimm, R. Meier, V. Ntziachristos, R. Haag, Polyglycerolsulfate Functionalized Gold Nanorods as Optoacoustic Signal Nanoamplifiers for In Vivo Bioimaging of Rheumatoid Arthritis, Theranostics 4 (6) (2014) 629–641.
- [20] C.C. Bao, N. Beziere, P. del Pino, B. Pelaz, G. Estrada, F.R. Tian, V. Ntziachristos, J. M. de la Fuente, D.X. Cui, Gold Nanoprisms as Optoacoustic Signal Nanoamplifiers for In Vivo Bioimaging of Gastrointestinal Cancers, Small 9 (1) (2013) 68–74.
- [21] J. Song, J. Kim, S. Hwang, M. Jeon, S. Jeong, C. Kim, S. Kim, “Smart” gold nanoparticles for photoacoustic imaging: an imaging contrast agent responsive to the cancer microenvironment and signal amplification via pH-induced aggregation, Chem Commun 52 (53) (2016) 8287–8290.
- [22] Y.S. Chen, W. Frey, S. Kim, P. Kruizinga, K. Homan, S. Emelianov, Silica-Coated Gold Nanorods as Photoacoustic Signal Nanoamplifiers, Nano Lett 11 (2) (2011) 348–354.
- [23] Y.P. Ye, X.Y. Chen, Integrin Targeting for Tumor Optical Imaging, Theranostics 1 (2011) 102–126.
- [24] Z. Liu, L. Yu, X. Wang, X. Zhang, M. Liu, W. Zeng, Integrin (alpha ν beta3) Targeted RGD Peptide Based Probe for Cancer Optical Imaging, Current protein & peptide science 17 (6) (2016) 570–581.
- [25] N. Beziere, N. Lozano, A. Nunes, J. Salichs, D. Queiros, K. Kostarelos, V. Ntziachristos, Dynamic imaging of PEGylated indocyanine green (ICG) liposomes within the tumor microenvironment using multi-spectral optoacoustic tomography (MSOT), Biomaterials 37 (2015) 415–424.
- [26] V. Neuschmelting, H. Lockau, V. Ntziachristos, J. Grimm, M.F. Kircher, Lymph Node Micrometastases and In-Transit Metastases from Melanoma: In Vivo Detection with Multispectral Optoacoustic Imaging in a Mouse Model, Radiology 280 (1) (2016) 137–150.
- [27] I. Stoffels, S. Morscher, I. Helfrich, U. Hillen, J. Lehy, N.C. Burton, T.C.P. Sardaella, J. Claussen, T.D. Poeppel, H.S. Bachmann, A. Roesch, K. Griewank, D. Schadendorf, M. Gunzer, J. Klode, Metastatic status of sentinel lymph nodes in melanoma determined noninvasively with multispectral optoacoustic imaging, Sci Transl Med 7 (317) (2015).
- [28] R.M. Huang, J. Vider, J.L. Kovar, D.M. Olive, I.K. Mellinghoff, P. Mayer-Kuckuk, M. F. Kircher, R.G. Blasberg, Integrin alpha ν beta3)- Targeted IRDye 800CW Near-Infrared Imaging of Glioblastoma, Clinical Cancer Research 18 (20) (2012) 5731–5740.
- [29] U.K. Marelli, F. Rechenmacher, T.R. Sobahi, C. Mas-Moruno, H. Kessler, Tumor Targeting via Integrin Ligands, Frontiers in oncology 3 (2013) 222.
- [30] J.S. Desgrosellier, D.A. Cheresch, Integrins in cancer: biological implications and therapeutic opportunities, Nature Reviews Cancer 10 (1) (2010) 9–22.



treatment procedures.

Dr. Katja Haedicke studied Microbiology in her Master at the Friedrich-Schiller University of Jena and received her PhD in 2015 at the Jena University Hospital from the department of Experimental Radiology under the supervision of Prof. Dr. Ingrid Hilger. During this time, she focused on evaluating the therapeutic efficacy of photodynamic therapy by means of fluorescence optical imaging. In 2015, she started to work as a postdoctoral Research Scholar in the lab of Prof. Dr. Jan Grimm at Memorial Sloan Kettering Cancer Center in New York. Here, she is working on imaging modalities like photoacoustic and Cerenkov imaging to get better insights into tumor biology and therapies and to improve cancer



Dr. Christian Brand received his PhD in 2012 from the University of Goettingen, Germany, where he was trained as a synthetic organic chemist. After a short postdoc at the University of Goettingen as an organic chemist, he joined the group of Prof. Dr. Thomas Reiner as a postdoctoral Research Scholar at Memorial Sloan Kettering Cancer Center, New York. His focus as a radiochemist lies in the development and translation of novel radiopharmaceuticals for the diagnosis of cancer.



Dr. Murad Omar received his PhD in electrical engineering from the Technical University of Munich in 2015. Currently, he is a postdoctoral researcher and group leader at the Institute for Biological and Medical Imaging of the Technical University Munich and the Helmholtz Zentrum in Munich, Germany, where he works on the development of optoacoustic mesoscopy, image reconstruction methods, and data analysis tools for biomedical imaging.



Professor Vasilis Ntziachristos received his PhD in electrical engineering from the University of Pennsylvania, USA, followed by a postdoctoral position at the Center for Molecular Imaging Research at Harvard Medical School. Afterwards, he became an Instructor and following an Assistant Professor and Director at the Laboratory for Bio-Optics and Molecular Imaging at Harvard University and Massachusetts General Hospital, Boston, USA. Currently, he is the Director of the Institute for Biological and Medical Imaging at the Helmholtz Zentrum in Munich, Germany, as well as a Professor of Electrical Engineering, Professor of Medicine and Chair for Biological Imaging at the Technical University Munich. His work

focuses on novel innovative optical and optoacoustic imaging modalities for studying biological processes and diseases as well as the translation of these findings into the clinic.



Professor Thomas Reiner received his PhD in 2009 from the Technical University of Munich, Germany, where he was trained as a synthetic chemist. After graduation, he accepted a position as a postdoctoral fellow at the Center for Systems Biology at Massachusetts General Hospital under the mentorship of Ralph Weissleder. In 2012, he transferred to Memorial Sloan Kettering Cancer Center as an Assistance Professor, where he and his group are investigating and translating novel types of tracers and imaging methodologies, always with the aim of improving the current standard of care.



Professor Jan Grimm received his MD from the University of Hamburg and his PhD from the University of Schleswig-Holstein, Germany. He was a postdoctoral fellow and later faculty at the Center for Molecular Imaging Research at Massachusetts General Hospital, Boston, until 2006. Currently, he is Associate Member of the Molecular Pharmacology Program in the Sloan Kettering Institute, Associate Attending at Memorial Hospital, and Associate Professor at the Gerstner Sloan Kettering Graduate School of Biomedical Sciences, all of Memorial Sloan Kettering Cancer Center. He is also faculty in Radiology and Pharmacology in Weil Cornell Medical College. His lab focuses on the development of novel innovative imaging and therapy approaches for cancer diagnostics, such as Cerenkov Imaging, and strives to develop novel concepts on how to image biological

events, including basic biology while simultaneously keeping clinical translatability within sight. His clinical focus is on body and nuclear imaging. He is board certified in Radiology (Germany and US) and Nuclear Medicine (US).